Response to Reviewers

Response to Referee 1

The authors show the results of an experiment dealing with Raman Scattering and fluorescenceaiming studying aerosol properties. Innthis study a set of different scenarios are shown aiming to verify how meteorlogical conditions might affect the overall results. Also the presence of clouds were inspected. The experimental setup is well explained as well the theory involved in making this experiment. Given all this aspects I consider the paper is well suited for thi journal and reaches all the needed publication standards.

We are grateful to the reviewer, for reading the manuscript and for appraisal of our work.

Response to Referee 2

First of all, we would like to thank the reviewer for careful the manuscript and for numerous useful suggestions. In revised manuscript we changed the structure, adding more information in about fluorescence in Introduction. We also revised the chapter, containing analysis of particle fluorescence in the cloud.

Below we provide detailed response to the reviewer comments

General: The paper contains new and very interesting observations obtained with a new approach of a fluorescence lidar for aerosol characterization. This lidar feasibility study is clearly worthwhile to be published in AMT. Nevertheless, the interpretation of the observations needs to be improved. A clear and more systematic separation of the different fluorescence contributions would be helpful to better follow the discussion. The argumentation is partly week and a bit speculative. Minor revisions are requested.
The abstract has to be updated and adjusted : after all the suggested improvements.

Abstract is revised

P2, L39: Burton et al. 2012: : : Only one reference here? What about own papers:Dscussion paper
Veselovskii et al., 2015, 2020, what about Tesche 2011, Tellus, SAMUM 2, what about
all the efforts within the ACTRIS EARLINET group on aerosol typing: : : during the last
five years.
In revised manuscript we added:

e.g. Tesche et al., 2011; Burton et al., 2012, Luís Guerrero-Rascado et al., 2018; Veselovskii et al., 2020 and references therein

Definitely, there are a lot of important papers, showing potential of lidar technique for aerosol studies. We just can't mention them all, because we focus of fluorescence measurements.

P2, L44-47: I have my doubts that aerosol particles can be clearly identified and quantified in cloud layers. Ok, you can detect them, but it is already well known that interstitial aerosol particles are always present in clouds. It is impossible to have aerosol particle free clouds.

P3, L76-84: These are confusing statement. I am puzzled by the wording ..'external' vs 'internal' mixing of aerosol particles within liquid water droplets. There is only ONE scenario: It is impossible to have droplets without a CCN, and it is also impossible to have clouds without interstitial aerosol particles (non-activated particles). So, there is only this ONE scenario: a mixture of interstitial aerosol particles (not acting as CCN) and droplets, each of the droplets nucleated on a CCN. The CCNs may be completely dissolved in the droplet, or survived as a solid particle within the droplet, as is the case for dust or soot CCN.

The interstitial aerosol particles (in the cloud) may be much larger than the particles outside the cloud (because of strong water uptake at 100% rel. humidity), so the aerosol backscatter efficiency of particles within the cloud may be larger by a factor of 5 and even more, compared to the aerosol backscatter outside the cloud layer.

I recommend to avoid to introduce : internal and external mixtures! There is only this ONE scenario: interstitial aerosol particles and cloud droplets. Now we need a clear differentiation: What is the contribution of dry particles to fluorescence? What is the contribution of fully deliquescent (dissolved, solution) aerosol particles? Sulfate particles are fully dissolved at high humidities? Can we be sure that the fluorescence signal in clouds is exclusively from interstitial aerosol particles? No contribution by cloud droplets? That needs to be carefully discussed.

This is important comment and we agree with reviewer. In revised manuscript we don't use "internal or external mixture". Numerous modifications are introduced in the text. In particular, in Introduction we added paragraph:

"Interpretation of fluorescent measurements in a cloud is even more challenging. The liquid cloud is a mixture of interstitial aerosol particles (non-activated particles) and droplets, formed on the cloud condensation nucleus (CCNs). The CCNs may be completely dissolved in the droplet, or survived as a solid particle within the droplet, as is the case for dust or soot. The relative contributions of interstitial aerosol and activated CCNs in the droplets to the total cloud fluorescence backscatter are unknown, and the need to estimate these contributions was one of the motivations of this study"

Dust particles with liquid shell : : :. produce an enhanced fluorescence signal (lens rdly version effect)! Is that checked? Is there a reference for that?

To our knowledge, nobody discussed lens effect in respect to fluorescence. But physically, it may take place.

P5, L157: Please keep in mind that RH increases from dry conditions (e.g., RH of 40%) to moist conditions (e.g., 80%, 90%, 95%) already a few hundred meters below cloud base, and then to 100% above cloud base. The aerosol particles grow by water uptake, change their backscatter efficiency and the fluorescence capability, some get *liquid, some remain dry.*

Yes, influence of RH on fluorescence is a principal question. It strongly influences elastic scattering, but fluorescence is altered much less. We added paragraph in Introduction:

"One of the factors that intricate obtaining the quantitative information about aerosol properties from fluorescence measurements, is influence of the relative humidity (RH). The aerosol particles grow by water uptake, changing their elastic scatter cross-section, but the change in water percentage within an aerosol particle, normally does not alter the chemical components, so total amount of fluorescent molecules within a particle does not change. However the illumination intensity distribution within a particle, as well as the emission angle distribution will be altered by the change of particle size, shape and refractive index, and this modification may affect the fluorescence measurement. The phase functions of the microspheres for the incoherent scattering (fluorescence is an example of incoherent scattering), were computed in works of Kerker and Druger (1979) and Veselovskii et al. (2002a). Results demonstrate, that fluorescence of particles dissolved in water microspheres can be increased in the backward direction by factor ~2, comparing to fluorescence of a bulk material (calculated per gram of solid matter). This enhancement, however, occurs for relatively big microspheres with size parameter $x = \frac{2\pi r}{\lambda}$ exceeding approximately 10 (Veselovskii et al., 2002a). For the wavelength λ=532 nm corresponding radius r is about 1.0 µm, so fluorescence of the fine mode particles should be affected less by the hygroscopic growth. We should mention also that for insoluble particles, the presence of the water shell, at the condition of high RH, in principle, can lead to an additional increase of the fluorescence, due to the water droplet lens effect. Similar effect is well known for the soot particles covered by non-absorbing shell (Schnaiter, 2005)."

Then in the cloud, cloud droplets come into play, backscatter efficiency of interstitial aerosol particles (at 100% humidity) may be much larger than for the aerosol particles below the cloud, or before the cloud formed. All this needs to be considered: : : in the cloud observations of backscatter and fluorescence signals.

As we mentioned, fluorescence is less altered by droplets formation than elastic scattering. Estimated (from numerical modeling) increase of fluorescence backscattering should be about factor 2.Fig. 8a demonstrates that fluorescence of aerosol in the cloud increases about twice, when elastic backscattering is increased above 3 orders.

Is all this known well enough to quantify the aerosol-related (non-droplet) fluorescence signal in clouds? To my opinion this is not the case. We do not know much about this. So, I have my doubts about Eq.(7).

Definitely, there are a lot of questions, when we try characterize aerosol inside the cloud from fluorescence. Still we think, that for the aerosol outside of the cloud such estimations can be done, at least at the condition of low RH. Corresponding comment is added to the manuscript.

P6, L176, the particle fluorescence capacity is introduced. I would recommend to do that in form of an equation.

Done

Now, the fluorescence signal will change with increasing humidity and water uptake and this in a different way as the total backscatter signal. Again, I think the knowledge about water uptake and the link to fluorescence signal changes is just qualitative. So there is no clear knowledge about the increase of the capacity G with water uptake:

We agree, that altering the fluorescence by water uptake is not completely understood and results, at least for the clouds, are qualitative. Corresponding comments are added to the text..

P6, L176, beta_L ˆa is introduced in Eq. (1) but not beta_L or betaˆa.

Yes, but on page 7 we write "Here and below, for simplicity, we will use notation a β β ≡ ." So we think here is no misunderstanding.

P6, L176: The capacity G_F expresses what? The fluorescence signal changes probably when aerosol particle get a wet coating, the backscatter signal changes by water uptake, so there is no clear reference (denominator), and thus, what does G_F indicate?

For the fine mode particles water uptake should not alter significantly fluorescence backscattering. For example, on 29-30 November variation of RH from 70% to 20% is accompanied by decrease of elastic scattering by factor 40 while fluorescence backscattering is decreased less than twice. So drop of fluorescence capacity is directly related with water uptake and this is important parameter when we compare different aerosols at low RH. Besides, at low RH the fluorescence capacity is used to compare fluorescent properties of different aerosol types.

P6, L185 and L187: Again, because of the not well-known impact of water uptake, I do not believe that you can quantify N and V at conditions with rising humidity just below cloud base or even within the cloud? : So that you can not estimate fluorescence cross sections accurately enough. If you want to present it please clearly state that there are many questions how trustworthy this estimation is.

In the revised manuscript we describe the challenges of interpretation the fluorescence measurements. Estimations of the fluorescence cross section are presented only for low RH, when water uptake does not alter the results.

3. Observations:
A general comment: Trajectory analysis would be helpful for all cases discussed. There is no need to show them all, but it would improve the discussion .... to know more about the origin of air masses, and the kind of aerosol mixtures

Trajectory analysis is added.

And it would also be helpful to have something like a bullet point list or an overview table, what aerosol produces fluorescence, what does not cause fluorescence, the same for droplets or water in aerosol particles, what is producing fluorescence, and what does not. And please provide references that support these statements I ask for such a table because I learned more and more about fluorescence in detail :from page to page of the manuscript, without having a complete *picture right in the beginning of the discussion. Such an overview would facilitate all discussions and complex interpretation of the shown observations.*

In revised manuscript we moved the information about fluorescence measurements to the Introduction, which should facilitate the process of manuscript reading. We wouldn't like to provide the table, because the information about fluorescence of different atmospheric aerosols in ambient conditions is quite rare. For the same reason it is not easy to support our conclusions with references: there are quite few publications on fluorescence lidars, providing quantitative results.

P7, L205-206: Do you mean external mixing of dust and biological /organic particles, or do you mean internal mixing, this would mean coating or partly coating of dust particles with organic material.

It can be both. Unfortunately, at this stage we can not separate these two possible scenarios.

P7, L215: Pure water is not fluorescing, but what about the aqueous solution of dissolved aerosol particles (before becoming a droplet when acting as CCN). Again, what about the change in fluorescence efficiency with increasing water uptake and finally even change of phase (from dry and solid to totally liquid-acid aerosol particle)?

Dissolved aerosol particles should provide the fluorescence. From our expectations, fluorescence efficiency in dissolved state should be increased by approximately factor 2. However, in some measurements, when cloud was formed at the top of aerosol layer, this enhancement was up to factor 5. At a moment we can not identify the mechanisms, responsible for such strong enhancement.

P8, in general and to mention again: would be nice to have HYSPLIT backward trajectories to learn more about aerosol mixtures observed and what kind of aerosol are candidates for causing significant fluorescence.

HYSPLIT analysis is added

P9, L266-280: Again the discussion part with N and V, I am not convinced that this is a fruitful part. Yes, there are numbers, but can we trust them?

We think, that such estimations can be used, at least for low RH. We compared results of such estimations with regularization inversion and agreement is reasonably good.

Discussion paper
3.2. Fluorescence of aerosol particles within clouds This section is very interesting but, at the same time, a bit confusing. A more systematic way of presentation would be useful: What causes fluorescence, what not, what is the impact of water uptake, what happens with fluorescene when droplets are formed, with 'liquid' CCN and with solid CCN, etc. So, a bullet point list or a Table would be nice. We added a section in Introduction, trying to explain these issues.

The section is strongly modified and some of unsupported statements are removed.

P10, L290-299: Again, this separation of externally and internally mixed cloud: As mentioned above, there is only ONE scenario: In all clouds, there is just a mixture of interstitial aerosol particles (not acting as CCN) and cloud droplets nucleated on the available CCNs. Furthermore: In the cloud we have 100% relative humidity, so the interstitial aerosol articles are not dry, and most of them are just solution droplets (before activation to become cloud droplets). And the water droplets, on the other hand side, are formed on part of the solution droplets (CCN) but now consist almost entirely of water. So please rephrase, and avoid external and internal mixing

We agree with reviewer. “Internal or external mixing” is not used in the revised manuscript.

P10, L311: What do you mean here? Fluorescent aerosol particles are inside the water particles. Ok, but must they be solid? If they are dissolved in the aqueous solutions, will there still be a fluorescene signal? May be droplets and CCN in the droplet do not produce any fluorescence signal, and fluorescence is only caused by the interstitial aerosol particles, and the increase in the fluorescence signal arises from water uptake effects?

We think that dissolved CCN provides the fluorescence signal. As mentioned, in dissolved state the signal should be about factor 2 stronger than in solid. Still this signal is probably rather week. In particular, Fig.8b demonstrates, that fluorescence of the cloud at 2500 m is low, when the aerosol below the cloud base is not detectable. This is in contrast with results in Fig.8a, where strong fluorescence is probably provided by interstitial aerosol

So, what shows Fig4? in contrast to Fig5? If there is a difference, what is the reason?

In Fig.4 oscillations of elastic backscattering don’t lead to synchronous oscillations of fluorescence, while in Fig.5 they do. We have no ultimate explanation for such difference, but looks like in Fig.5 the vapor is condensed in the aerosol layer, while in Fig.4 the weak water cloud layers are just mixed with aerosol.

P11, L322: Please, do not switch from one wavelength to another. That makes comparisons confusing. If beta1064 is 0.07 Mm-1 sr-1, then the 532 nm backscatter coefficients below the cloud is probably about 0.15 to 0.2 Mm-1 sr-1. That should be mentioned. And then we have an increase by a factor of roughly 3000 when you measure cloud a cloud beta532 value of 500 Mm-1 sr-1, and the fluorescence signal increases just by a factor of 5. that is a good proof that water does not produce a fluorescence contribution. Please state that, if my comment is true, and if there is definitely no cross talk:

In revised manuscript we provide backscattering at 532 nm prior and after cloud formation. We believe that there is no cross talk, because we had observations (e.g. Fig.8b) with strong cloud backscattering, which were not accompanied by increase of fluorescence.

P11, L327-328: Again almost the same increase in beta 532 when we start from about 0.04 Mm-1 sr-1 for 532nm (estimated from 1064 nm information) and end up at 130 Mm-1 sr-1. All this should be given in more clearly way : : : by using ONE wavelength.

Done

But can we trust an increase by factor 5 of the aerosol-related fluorescence backscatter when the elastic backscatter increase by a factor of 3000? Can we be sure that there is no cross talk, not stray light somewhere, nothing?

We believe that there is no cross talk, because we had observations (e.g. Fig.8b) with strong cloud backscattering, which were not accompanied by increase of fluorescence.

What causes the increase? The lens effect? Is there another explanation?

At a moment we can not identify the mechanism

P11, L342 For insoluble particles increase of fluorescence by lens effects. Yes that can be, but it remains speculations, most of urban aerosol is sulfate aerosol (and not BC-containing haze) and sulfate particles dissolve completely and then there is no lens effect

Yes, we can not prove it so we just mention such possibility. To our knowledge nobody considered lens effect in respect to fluorescence. But physically this is possible, for example for soot or dust particles covered by water shell. And definitely no lens effect for dissolved aerosol.

P12, L358-362: This is again a non-acceptable speculation. The two cloud layers may have formed in two different air masses with different aerosol types, and the different aerosol types caused different levels of fluorescence.

Yes, we agree that two cloud layers can be different. We just wanted to emphasize, that in some cases aerosol fluorescence in the cloud is very low (Fig.8b), while in others fluorescence is strong (Fig.8a), meaning significant content of aerosol in the cloud.

Figure 2, would be nice to have backward trajectories: : : and thus origin of air masses for the two cases.

We added information about back trajectories in the text.

Figure 3, again: what is the origin of the aerosol (according to HYSPLIT trajectories)?

HYSPLIT analysis is added

Figure 4, strong increase of cloud beta532 but not of fluorescence beta, what can we conclude? Strong increase of beta532 by droplet backscatter, and at least significant increase of the fluorescence signal because of water uptake of interstitial particles

We think that cloud layers, characterized by small content of aerosol (and so by low fluorescence), are mixed with aerosol particles. High RH in these layers doesn’t alter significantly the fluorescence efficiency of aerosol, so oscillations of elastic backscattering is not accompanied by synchronous oscillation of fluorescence.

And again, HYSPLIT trajectories would be nice to all the cases discussed. The trajectories must not be shown in detail, but information about origin and mixture of aerosol particles would be helpful.

We added HYSPLIT analysis in the text for cases with clouds and elevated aerosol layers.

Final remark: This is a good paper and needs only some minor clarifying information and a clear definition of the cloud environment (with interstitial non-CCN aerosol particles and CCNbased cloud droplets). Afterwards (in the comparison: : :before vs within the cloud) a clear definition and systematic separation of the contributions by dry aerosol particles, wet aerosol particles, dissolved aerosol particles, cloud droplets nucleated on sulfate aerosol, and cloud droplets formed on soot and dust particles to fluorescence and to backscatter would be good and would make the discussion easier.

We tried to follow these suggestions in the revised manuscript.

Response to Referee 3

First of all, we would like thank the Reviewer for careful reading our manuscript and suggestions. Below are responses to his comments.

Summary: The manuscript reports on fluorescence measurements of atmospheric aerosols with a multi-wavelength Raman lidar, where the interference filter in the water vapor Raman channel was replaced by a broadband filter around 466 nm. Although the study contains some interesting approaches, e.g. the possible synergy of combined measurements with multi-wavelength Raman lidar and fluorescence lidar, it is incomplete and too speculative at this stage and requires substantial extensions and improvements for a possible publication. For example, it is incomprehensible why the authors do not present aerosol events that could show the real strength of their modified lidar system (microphysical retrieval plus fluorescence), but only those that are actually not suitable. A little more patience would have been necessary here.

As mention by the Reviewer, combining the multiwavelength and fluorescence measurements can be a promising approach for aerosol characterization. But to implement it, some important questions should be answered first. These questions, in particular, are:

- Is fluorescence technique sensitive enough to be useful for lidar aerosol measurements, when part of the spectrum is selected by the interference filter?
- How the fluorescence signal is affected by the variation of the relative humidity and by the droplets formation?
- Is it possible to measure the fluorescence signal inside the cloud layer?

In our manuscript we tried to get answers for these questions and to demonstrate the feasibility of our system for fluorescence studies.

By today we have measurements performed during high aerosol loading, and combining of multiwavelength retrievals with fluorescence data is in progress. However this is a subject of separate study. We wouldn't want to add multiwavelength inversion to this one.

We should recall also, that when aerosol near the cloud base is considered, usually the aerosol extinction coefficients are quite low and traditional multiwavelength Raman technique does not work. In our study we consider cases with low aerosol loading and suggest approach, based on use of predefined aerosol models, for aerosol characterization.

Furthermore, the paper shows technical weaknesses in both the experiment and the analysis, and the interpretation of the measurements is highly speculative. For example, the fluorescence measurement has not been thoroughly calibrated,

Equation (9) for the fluorescence backscattering contains the ratio of efficiencies of fluorescence and Raman channels. The dichroic optics used, allows efficient separation of fluorescence and Raman signals, so main source of uncertainty is relative sensitivity of PMTs in the channels. To equalize sensitivities, the PMT from fluorescence channel was installed in the Raman one and by small adjusting of voltage the same value of nitrogen Raman signal was obtained. The cathode sensitivity of R9880U-01 PMT between 387 nm and 466 nm changes for less than 15%, thus we assume that sensitivities of PMTs in both channels are the same and only difference in transmission of interference filters was considered. We estimate that uncertainty of such calibration is less than factor 2, which is sufficient for our purpose, because relative variations of fluorescence backscattering coefficient are considered. Corresponding comment is added to the text.

and no backward trajectories were used for aerosol typing.

In revised manuscript we discuss backward trajectories

Furthermore, the measurement results are discussed using relative humidity, although neither water vapor measurements with the lidar nor local radiosondes were available.

Yes, RH data were available only from radiosond in Belgium (95 km away). However in this study we don’t analyze the hygroscopic growth. RH data are taken as qualitative only.

Interestingly, the authors themselves point out some of these weaknesses in their conclusions, they should fix them and then resubmit the manuscript.

We definitely understand all these weak points, still we think that this study presents new important results.

Major issues:

1. The calibration of the lidar was not performed with a spectral lamp (l. 169 ff), so the measurement trueness is questionable, and the authors are aware of this (l. 380 ff). Why was the calibration not performed? Nevertheless, the measurements are quantitatively evaluated and interpreted, this is not a consistent approach.

We have already responded this comment. Discussing the cross sections obtained, we emphasize, that these are only rough estimations.

2. The authors speculate about the presence of aerosol mixtures (l. 204 ff). This can only be investigated with spectrometric fluorescence lidars, if at all. But at least an analysis of the backward trajectories should have been performed.

In revised manuscript we added back trajectory analysis. Air masses pass Africa and particle depolarization ratio is high. So dust is predominant in aerosol mixture.

This also applies to the statements regarding the change of GF (l. 225 ff).

We are not able indentify aerosol type for this case

3. Relative humidity is used for the interpretation of the measurements, although it is not known sufficiently for these purposes, especially for hygroscopic aerosol growth (l. 211 ff). Thus the interpretation is a speculation.

We don’t analyze hygroscopic growth. We just say that RH is high at 1000 m and drops above 2000 m. The sonde data from England and from Belgium lead to similar conclusion.

4. Particle depolarization is not only a function of particle shape but also of particle size, this should be considered in the discussion.

Yes, depolarization definitely depends on particle size. But here we focus on the fluorescence. Analysis of dependence of depolarization on particle parameters is out of the scope of this study.

5. The whole microphysical interpretation (l. 244 ff) is pure speculation. Why did the authors not wait for aerosol measurement cases where they could have used the strengths of their multi-wavelength Raman lidar?

In situations, when aerosol extinction is low (for example when aerosol near the cloud base is analyzed) the multiwavelength Raman technique can not be used. So other approaches, allowing at least qualitative estimations of particle properties are needed. The estimations of particle properties, based on predefined aerosol models are widely used in remote sensing. In our study we used the aerosol models based on AERONET observations. Still we agree that such estimations need numerous assumptions, thus results obtained can be considered as qualitative only. Corresponding comments are added to revised manuscript.

Discussion paper

6. The reviewer is sceptical about the measurements in chapter 3.2, which are supposed to prove an internal mixture of aerosol particles and cloud droplets (l. 311 ff).

Reviewer 2 provided numerous comments, concerning “internal and external mixing”. So in revised manuscript we don’t use this terminology.

It is noticeable that the fluorescence signal associated with the cloud layers seems to be a function of the measurement height: below 1000 m very high ’fluorescence’ values are found in clouds, around 1500 m slight increases, and above 1700 m elastic and fluorescence signals are uncorrelated. This may (but of course does not have to) indicate instrumental effects (height-dependent angle-of-incidence distribution of the backscattered photons). Are there measurement examples where liquid water clouds below 1000 m do not show increased fluorescence?

Yes, reviewer is right, height dependence of fluorescence is complicated and depends on aerosol loading. We think that this is result of water uptake by aerosol (aerosol dissolving, water shell forming…). We don’t see how instrumental effects can result in such profiles, because we had many aerosol observations without such “exotic” behavior at low altitudes (Fig.6 in this manuscript). Still in the presence of high RH elastic scattering and fluorescence don’t correlate, because water uptake by particles normally does not increase fluorescence significantly.

Minor issues:

1. The authors claim that lidars with spectrometers are less sensitive than those with standard detection channels (l. 61 ff). However, a comparison with published spectrometric measurements seems to contradict this. Please explain in more detail.

Transmission of the interference filters used is above 95%, while transmission of grating spectrometer with fiber input is definitely lower. This why we say that spectrometer is less sensitive. In revised manuscript we modified this phrase as

“However, sensitivity of such lidar spectrometers is lower when compared to the technique based on selection of fluorescence spectrum intervals with interference filters, because the transmission of modern filters exceeds 90%”.

2. The authors plan to reduce the bandwidth of the interference filter for fluorescence measurements by a factor of 2 or even 4 in the future (l. 404 ff). However, this would further increase the measurement duration, which is already very long. Please explain in more detail.

In Fig.2 we show fluorescence maps obtained with 2 min resolution at low aerosol loading. So we have resource to reduce the filter width. But our experience of fluorescence measurements (and data analysis) shows that we never have “too much” signal. So the phrase about bandwidth reduction is removed from revised manuscript.

Wording:

1. To speak of a ‘highly efficient lidar operation’ (l. 368) when in fact hour-long integration times are needed for fluorescence measurements is quite a stretch.

Changed for “efficient”

Type setting:

1. All variables in the running text and in the equations must be checked for correct math format. There are many formatting errors, for instance, variables are not italic (e.g., l. 133), or subscripts are italic (e.g., l. 119).

Changed

1. Figures 1 and 7 are of poor quality.

Why? We don’t think that these are of poor quality…

2. Figure 6, colors for beta_1064 and beta_F are hardly distinguishable when printed.

We changed color of beta 1064 line for blue.

Combined use of Mie-Raman and fluorescence lidar observations for improving aerosol characterization: feasibility experiment

Igor Veselovskii[1], Qiaoyun Hu[2], Philippe Goloub[2], Thierry Podvin[2], Mikhail Korenskiy[1], Olivier Pujol[2], Oleg Dubovik[2], Anton Lopatin[3]

[1]Prokhorov General Physics Institute of the Russian Academy of Sciences, Moscow, Russia.

[2]Univ. Lille, CNRS, UMR 8518 - LOA - Laboratoire d'Optique Atmosphérique, Lille F-59000, France

[3]GRASP-SAS, Villeneuve d'Ascq, France

Abstract

To study the feasibility of a fluorescence lidar for aerosol characterization, the fluorescence channel is added to LILAS - multiwavelength Mie-Raman lidar of Lille University, France. A part of fluorescence spectrum induced by 355 nm laser radiation, is selected by the interference filter of 44 nm bandwidth centered at 466 nm. Such an approach has proved high sensitivity, allowing to detect fluorescence signals from weak aerosol layers and to calculate the fluorescence backscattering coefficient from the ratio of fluorescence and nitrogen Raman backscatters. Observations were performed during November 2019 – February 2020 period. The fluorescence capacity (ratio of fluorescence to elastic backscattering coefficients), measured at the condition of low relative humidity, varied in a wide range, being the highest for the smoke and the lowest for the dust particles. The results presented demonstrate also, that the fluorescence measurements can be used for monitoring the aerosol inside the cloud layers.

1. Introduction

The aerosol – cloud interaction is one of the key factors influencing the Earth radiation balance and, for its realistic modeling, knowledge of aerosol properties both outside and within the cloud layer are needed. The multiwavelength Mie-Raman and HSRL lidars, measuring aerosol backscattering and extinction coefficients at multiple wavelengths, are widely used for remote characterization of aerosol properties (e.g. Tesche et al., 2011; Burton et al., 2012, Luís Guerrero-Rascado et al., 2018; Veselovskii et al., 2020 and references therein). However, although useful for studying aerosol, the amount of information contained in these measurements remains limited (Burton et al., 2016; Alexandrov and Mishchenko, 2017). In addition, such lidars are not able to detect and characterize aerosol inside a cloud layer, because aerosol scattering is masked by the strong cloud particles scattering. To improve the lidar capability for aerosol characterization, additional channels, measuring the laser induced fluorescence, can be used.

Fluorescence spectroscopy is a highly sensitive technique, widely used for the in-situ monitoring of atmospheric organic particles (Pan et al., 2007, 2015; Miyakawa et al., 2015; Huffman et al., 2019). The synergy of fluorimetry and lidar technology provides an opportunity to perform such monitoring remotely (Immler et al., 2005; Rao et al., 2018; Saito et al., 2018). Numerous types of atmospheric aerosols, such as biological, biomass burning particles, sulfates and even dust are fluorescent, being excited by UV radiation. When the excitation wavelength is 355 nm, the main part of emission spectra is usually contained within the 400–650 nm range (Pan et al., 2015). The fluorescence spectrum varies with the aerosol types/composition, making therefore possible their identification. Moreover, due to the fact that pure water does not fluoresce, the measurement of cloud fluorescence allows to get information about aerosol particles within cloud layer, at least near the cloud base, thus allowing to investigate the aerosol – cloud coexistence.

One of the factors that intricate obtaining the quantitative information about aerosol properties from fluorescence measurements, is influence of the relative humidity (RH). The aerosol particles grow by water uptake, changing their elastic scatter cross-section, but the change in water percentage within an aerosol particle, normally does not alter the chemical components, so total amount of fluorescent molecules within a particle does not change. However the illumination intensity distribution within a particle, as well as the emission angle distribution will be altered by the change of particle size, shape and refractive index, and this modification may affect the fluorescence measurement. The phase functions of the microspheres for the incoherent scattering (fluorescence is an example of incoherent scattering), were computed in works of Kerker and Druger (1979) and Veselovskii et al. (2002a). Results demonstrate, that fluorescence of particles dissolved in water microspheres can be increased in the backward direction by factor ~2, comparing to fluorescence of a bulk material (calculated per gram of solid matter). This enhancement, however, occurs for relatively big microspheres with size parameter $x=\frac{2\pi r}{\lambda}$ exceeding approximately 10 (Veselovskii et al., 2002a). For the wavelength λ=532 nm corresponding radius r is about 1.0 µm, so fluorescence of the fine mode particles should be affected less by the hygroscopic growth. We should mention also that for insoluble particles, the presence of the water shell, at the condition of high RH, in principle, can lead to an additional increase of the fluorescence, due to the water droplet lens effect. Similar effect is well known for the soot particles covered by non-absorbing shell (Schnaiter, 2005).

Interpretation of fluorescent measurements in a cloud is even more challenging. The liquid cloud is a mixture of interstitial aerosol particles (non-activated particles) and droplets, formed on the cloud condensation nucleus (CCNs). The CCNs may be completely dissolved in the droplet, or survived as a solid particle within the droplet, as is the case for dust or soot. The relative contributions of interstitial aerosol and activated CCNs in the droplets to the total cloud fluorescence backscatter are unknown, and the need to estimate these contributions was one of the motivations of this study.

The recent interest in fluorescence lidars was stimulated also by the progress in the development of the multianode photomultipliers allowing, in combination with spectrometer, simultaneous detection of lidar signal in 32 spectral bins (Sugimoto et al., 2012; Reichardt et al., 2014, 2017; Saito et al., 2018). Such multichannel detection has the obvious advantage to analyze the whole spectrum, allowing the aerosol identification. However, sensitivity of such lidar spectrometers is lower when compared to the technique based on selection of fluorescence spectrum intervals with interference filters, because the transmission of modern filters exceeds 90%. The use of interference filters, in addition to being more sensitive, allows more affordable modification of a multiwavelength Mie-Raman lidar by adding one or more fluorescence channels. To obtain the highest sensitivity, it is mandatory to acquire the fluorescence in a wide spectral range which, however, makes the data analysis more complicated, because variation of aerosol and molecular transmission within the detection spectral range has to be accounted for. In addition, in Mie-Raman multi-wavelength lidars one should avoid the spectral intervals affected by elastic scattering and corresponding strong Raman lines.

In our paper we present the results of a feasibility experiment and evaluate the sensitivity of a single-channel fluorescence lidar. Measurements were performed at *Laboratoire d'Optique Atmosphérique* (LOA) during November 2019 – February 2020 period. During that period, the aerosol load was very low, so we were not able to determine the particle properties from multiwavelength observations. The objective was then to estimate the efficiency /added value of the fluorescence channel. We therefore mainly focus on analysis of efficiency of fluorescence lidar monitoring of different types of aerosol and on detection of aerosol particles inside low level cloud layers.

2. Experimental setup and data analysis

The measurements were performed using the LILAS - multiwavelength Mie-Raman lidar, based on a tripled Nd:YAG laser with a 20 Hz repetition rate and pulse energy of 70 mJ at 355 nm. The backscattered light is collected by a 40 cm aperture Newtonian telescope. The system is designed for simultaneous detection of elastic and Raman backscatters, allowing the so called $3\beta+2\alpha+3\delta$ data configuration, including three particle backscattering (β), two extinction (α) coefficients along with three depolarization ratios (δ). Description of the system can be found in recent publication of Hu et al., 2019. The aerosol extinction and backscattering coefficients at

355 and 532 nm were calculated from Mie-Raman observations (Ansmann et al., 1992) while backscattering at 1064 nm was derived by the Klett method (Klett, 1985).

For the experiment described, the system was modified: water vapor 408 nm Raman filter was replaced by a fluorescence one. Corresponding optical scheme together with transmission curve of the interference filter in the fluorescence channel are shown in Fig.1. The nitrogen Raman and fluorescence optical signals are separated by a dichroic mirror: more than 98% of 387 nm radiation is reflected and more than 95% of fluorescence signal is transmitted. For both nitrogen Raman and fluorescence channels, the R9880U-01 PMTs were used. A part of the wideband fluorescence signal was selected by an Alluxa interference filter centered at 466 nm with 44 nm bandwidth. The filter transmission, at maximum, exceeds 98%. The operational band was chosen outside of the overtones of O_2 and N_2 vibrational Raman lines. In addition, the transmission of the selected fluorescence filter band matches the maxima of fluorescence of many organic molecules (Saito et al., 2018; Reichardt et al., 2017). Filter provides OD6 suppression outside the transmission band. To increase the suppression, two identical interference filters were used in tandem. For additional rejection of elastic scattering at 355 nm and 532 nm the two-band notch filter was used. With such design, we estimate that the total suppression of elastic scattering in the fluorescence channel is above OD14. In this paper, observations were carried out during night-time only.

In an elastic channel, the backscattered radiative power P_L, at distance z is described by the lidar equation

$$P_L = O(z)\frac{1}{z^2}C_L(\beta_L^a+\beta_L^m)\exp\left\{-2\int_0^z(\alpha_L^a+\alpha_L^m)dz'\right\} = O(z)\frac{1}{z^2}C_L(\beta_L^a+\beta_L^m)T_L^2 \qquad (1)$$

Here O(z) is the geometrical overlap factor, which is assumed to be the same for elastic, Raman and fluorescence channels. C_L is the range independent constant, including efficiency of detection channel. T_L is one-way transmission, describing light losses on the way from the lidar to distance z at laser wavelength λ_L. Backscattering and extinction coefficients contain aerosol and molecular contributions: $\beta_L^a+\beta_L^m$ and $\alpha_L^a+\alpha_L^m$, where the superscripts "*a*" and "*m*" indicate aerosol and molecular scattering, respectively.

In a Raman channel, the backscatter radiative power, P_R , can be rewritten as:

$$P_R = O(z)\frac{1}{z^2}C_R\beta_R\exp\left\{-\int_0^z(\alpha_L^a+\alpha_R^a+\alpha_L^m+\alpha_R^m)dz'\right\} = O(z)\frac{1}{z^2}C_R\beta_R T_L T_R \qquad (2)$$

Here T_R is the atmospheric transmission at Raman wavelength λ_R. Raman backscattering coefficient is:

$$\beta_R = N_R \sigma_R , \tag{3}$$

where N_R is the number of Raman scatters (per unit of volume) and σ_R is the Raman differential scattering cross section in the backward direction. To account for spectral dependence of aerosol extinction, the Angstrom exponent γ is used:

$$\frac{\alpha_L^a}{\alpha_R^a} = \left(\frac{\lambda_R}{\lambda_L}\right)^{\gamma} \tag{4}$$

The aerosol backscattering and extinction coefficients can be computed from Mie – Raman lidar observations using equations (1-4), as shown by Ansmann et al. (1992).

In the case of the fluorescence, the emitted wavelengths are spread over wide spectral range, so the spectral dependence of aerosol and molecular extinction coefficients, inside the fluorescence band, should be considered. Moreover, the spectral differential fluorescence cross section $\frac{d\sigma_F}{d\lambda}(\lambda,r)$ depends on particle size (Hill, et al., 2015), so the particle size distribution $\frac{dN(r)}{dr}$, which is the number of particles with radii between r and $r+dr$ per unit of volume, has to be considered. The radiative power in the fluorescence channel within the spectral interval $[\lambda_{\min},\lambda_{\max}]$ is:

$$P_F = O(z)\frac{1}{z^2}T_L \int_{\lambda_{\min}}^{\lambda_{\max}} \int_{r_{\min}}^{r_{\max}} C_F(\lambda) \times \frac{dN(r)}{dr} \times \frac{d\sigma_F}{d\lambda}(\lambda,r) \times \exp\left\{-\int_0^z [\alpha^a(\lambda,z') + \alpha^m(\lambda,z')]dz'\right\} dr d\lambda \tag{5}$$

The spectral dependence of $C_F(\lambda)$ is determined mainly by the transmission of the interference filter in the fluorescence channel. If the filter spectral width $\lambda_{\max} - \lambda_{\min}$ is not very high, the procedure of data analysis can be simplified. The atmospheric transmission for fluorescence signal

$$T_F(\lambda) = \exp\left\{-\int_0^z [\alpha^a(\lambda,z') + \alpha^m(\lambda,z')]dz'\right\} \tag{6}$$

can be taken at wavelength λ_F, corresponding to the center of the filter transmission band $T_F(\lambda) = T_F(\lambda_F) \equiv T_F$. The filter transmission used (Fig.1) is close to rectangular and sensitivity of the PMT used doesn’t vary significantly within $[\lambda_{min}, \lambda_{max}]$ interval, which means the calibration constant C_F can be considered as spectrally independent. Expression (5) can be rewritten, by introducing the fluorescence backscattering coefficient β_F:

$$\int_{\lambda_{\min}}^{\lambda_{\max}} \int_{r_{\min}}^{r_{\max}} \frac{dN(r)}{dr} \times \frac{d\sigma_F}{d\lambda}(\lambda,r) dr d\lambda = \int_{r_{\min}}^{r_{\max}} \frac{dN(r)}{dr} \times \sigma_F(r) dr = \beta_F \tag{7}$$

Here $\sigma_F(r)=\int\limits_{\lambda_{\min}}^{\lambda_{\max}}\frac{d\sigma_F}{d\lambda}(\lambda,r)d\lambda$ is the effective fluorescence differential cross section, integrated over spectral interval $[\lambda_{\min},\lambda_{\max}]$. The use of β_F allows to rewrite equation (5) for the power of the fluorescence backscattering similarly to the Raman one.

$$P_F=O(z)\frac{1}{z^2}C_F\beta_F T_F T_L \tag{8}$$

The fluorescence backscattering coefficient, β_F, can be obtained from the ratio of equations (8) and (2) for fluorescence and Raman backscatters:

$$\beta_F=\frac{C_R}{C_F}\frac{P_F}{P_R}N_R\sigma_R\frac{T_R}{T_F} \tag{9}$$

The ratio of atmospheric transmissions at λ_R and λ_F wavelengths (T_R/T_F) can be calculated the same way as for water vapor measurements (Ansmann et al., 1992; Whiteman et al., 2006). In our study, for the nitrogen molecule we used Raman scattering cross section at 355 nm σ_R=2.1*10^{-30} cm^2 (Burris et al., 1992), but, to obtain absolute values of β_F, C_R/C_F ratio must be determined. This ratio can be found from calibration, performed by using a lamp with known spectrum, as it has been done for the Raman water vapor lidars (Venable et al., 2011), but at current stage, we use simplified approach for estimation of C_R/C_F. The dichroic optics used, allows efficient separation of fluorescence and Raman signals, so main source of uncertainty is relative sensitivity of PMTs in the channels. To equalize sensitivities, the PMT from fluorescence channel was installed in the Raman one and by small adjusting of voltage the same value of nitrogen Raman signal was obtained. The cathode sensitivity of R9880U-01 PMT between 387 nm and 466 nm changes for less than 15%, thus we assume that sensitivities of PMTs in both channels are the same and only difference in transmission of interference filters was considered. In all results presented below C_R/C_F=0.7 value was used.

To characterize the efficiency of the fluorescence respect to elastic scattering, it is convenient to consider also the particle fluorescence capacity,

$$G_F=\frac{\beta_F}{\beta_L}, \tag{10}$$

which is the ratio of fluorescence and aerosol elastic backscattering coefficients (Reichardt et al., 2017). Here and below, for simplicity, we will use notation $\beta^a\equiv\beta$. The aerosol loading in the atmosphere during the experiment was very low and, in order to decrease the interference of the Raleigh scattering, the backscatter at 1064 nm was mainly used for aerosol characterization, while for the cloud layers the backscattering coefficients at 355 and 532 nm were used as well.

Multiwavelengtn Mie-Raman lidar measurements allow estimation of the particle number density $N = \int_{r_{\min}}^{r_{\max}} \frac{dN(r)}{dr} dr$ as well as their total volume V (Müller et al., 1999; Veselovskii et al., 2002b), thus a mean fluorescence cross section per a single particle can be estimated as $\sigma_F^N = \frac{\beta_F}{N}$. Assuming, that in the simplest case, a fluorescence backscattering coefficient is proportional to the particle volume, we can estimate the fluorescence cross section per a unit particle volume as $\sigma_F^V = \frac{\beta_F}{V}$. Thus, synergy of Mie-Raman and fluorescence lidar measurements should allow remote characterization of the particle fluorescent properties. We should mention however, that estimation of σ_F^V makes sense only at low RH, because water uptake by the particle will alter results.

3. Observation results.

3.1. Fluorescence of aerosol layers.

The measurements reported were performed during November 2019 – February 2020 period at the Lille Atmospheric Observation Platform (https://www-loa.univ-lille1.fr/observations/plateformes.html?p=apropos) hosted by Laboratoire d'Optique Atmospherique, University of Lille, Hauts-de-France region. Two examples of measurement are presented in Fig.2 and are showing height–temporal distributions of the range corrected lidar signal (RCLS) at 1064 nm, of volume depolarization ratio (δ_{1064}), and of fluorescence backscattering coefficient (β_F), for the nights 29-30th November 2019 and 6-7th February 2020.

During the first night (left column in Fig. 2), aerosol layer is localized mainly below 2000 m. Though the aerosol loading is low above 2000 m (β_{1064}<0.01 Mm^{-1}sr^{-1}), it is well revealed by the enhanced depolarization ratio and the enhanced fluorescence backscattering coefficient. During the second night of observation (right column in Fig.2), a detached/isolated layer is observed at approximately 3000 m. This layer is characterized by high depolarization ratio (the particle depolarization ratio at 1064 nm in the center of the layer exceeds 15%), indicating to the presence of dust. An explanation of the observed increase of fluorescence signal could be mixing of mineral dust particles with organic materials (Sugimoto et al., 2012; Miyakawa et al., 2015) and local aerosol during transportation.

The time averaged profiles (β_{1064}, β_F, G_F) for these two nights, as well as for 16th January episode are shown in Fig.3. Backscattering coefficient β_{1064} was calculated by Klett method, assuming a lidar ratio S=50 sr. Due to low aerosol extinction value, the results are not sensitive to the choice of *S*. The HYSPLIT back trajectory analysis (Stein et al., 2015) demonstrates that on 30 November and 16 January the air masses, at 3500 and 5000 m height respectively, were transported from Canada, so could contain the biomass burning particles. While on 6-7 February the air masses at 3000 m arrived from South – West passing near Africa, thus containing the dust particles. The closest available radiosonde data are from the Herstmonceux (UK) and Ebbe (Belgium) stations, located 150 km and 95 km away from the observation site respectively. Data from both stations show that on the night 29-30 November 2019 the relative humidity (RH) was about 70% at 1000 m and dropped below 20% above 2000 m. The fine mode of the particle size distribution over the observation site is normally predominant inside the planetary boundary layer (PBL). Pure water is not fluorescing, so the water uptake by the fine particles, at the condition of high RH, is expected to yield an increase of elastic scattering without significant effect on the fluorescence emission. The aerosol backscattering β_{1064} on 29-30th November (Fig.3a) is 0.4 $Mm^{-1}sr^{-1}$ at 1000 m and decreases by a factor 40 at 1900 m, while β_F within this height range changes less than twice. This is supporting the assumption that the observed variation of aerosol backscattering in the PBL is mainly due to the change of the particle water fraction. The water uptake at low altitudes agrees with low values of the observed particle depolarization ratio δ^{p}_{1064}, which is below 0.5% at 1000 m. Within weak aerosol layer at the range 2500 – 4000 m, the particle depolarization δ^{p}_{1064} is about 5% and we observe the increase of fluorescence capacity G_F, with respect to the layer below 2000 m, up to $2.5*10^{-4}$. This increase of G_F in the 2500 – 4000 m layer can be due to the presence of another particles type, for example, biomass burning. From this episode, one can conclude that fluorescence backscattering, though being almost 4 orders lower than elastic one, can be reliably detected with our current lidar configuration.

On January 16th (Fig.3b), atmospheric RH also decreases with height, from about 80% at 1000 m to less than 20% above 2000 m, leading to an increase of G_F for more than one order of magnitude. Such variation of G_F within the PBL is probably also related to the particle water uptake, just like in Fig.3a. Aerosol backscattering increases above 3000 m and reaches its maximum value at 5000 m. Within 3000 m – 5500 m range, fluorescence capacity was about $2.5*10^{-4}$, which is higher than in the PBL.

On February 6-7th the aerosol loading in the PBL is very low (β_{1064}<0.003 $Mm^{-1}sr^{-1}$ at 1000 m) and RH from radiosonde at Herstmonceux is below 40% in the height range considered. At 3000 m, a dust layer is observed (Fig.3c). In the middle of this layer, fluorescence capacity is about $0.6*10^{-4}$ which is about factor 4 lower than in the elevated layers in Fig.3a,b. Still, significant value of G_F can indicate the presence of organic materials in the dust layer (Sugimoto et al., 2012).

As discussed in section 2, lidar measurements provide an opportunity to estimate the particle fluorescence cross section. For this, we need to know the particle number N and volume V density in the aerosol layer, which, in principle, can be determined from the multiwavelength lidar observations (Muller et al., 1999; Veselovskii et al., 2002b). In our case, however, due to very low aerosol loading the extinction coefficients could not be determined. Still, the rough estimations of the particle parameters can be done using the predefined aerosol model driven by only a few parameters. In our study we use a simplified approach, modeling aerosol as an external mixture of several aerosol components with predetermined properties. The definition of aerosol components is based on global multiyear AERONET observations (Dubovik et al., 2002) with some modifications. All aerosol types are described by a bimodal particle size distribution (PSD)

$$\frac{dV}{d\ln r} = \sum_{i=f,c} \frac{C_{V,i}}{\sqrt{2\pi}\sigma_i} \exp\left[-\frac{(\ln r - \ln r_{V,i})^2}{2\sigma_i^2}\right] \tag{11}$$

where $C_{V,i}$ denotes the particle volume concentration, $r_{V,i}$ is the median radius, and σ_i is the standard deviation. Subscripts f and c correspond to the fine and coarse mode respectively. The parameters of the number size distribution $\frac{dN}{d\ln r}$ can be obtained from (11) using the expressions from Horvath et al. (1990). Table 1 shows the model parameters for three aerosol types: biomass burning (BB), urban (UR) and dust (DU). From this model, the aerosol backscattering and extinction coefficients can be calculated at any wavelength. As mentioned above, due to low aerosol loading, we use only backscattering coefficient at 1064 nm, so Table 1 presents $\beta_{1064}^{N=1} = \frac{\beta_{1064}}{\int_{r_{\min}}^{r_{\max}} \frac{dN(r)}{dr} dr}$ - mean backscattering coefficient for a single particle (N=1), together with corresponding complex refractive index (CRI) used in computations. Calculations were performed in assumptions of spherical particles for BB and UR and for the randomly oriented spheroids for dust (Dubovik, et al., 2006). The volume $V^{N=1}$ in the Table 1 is also given for N=1 (so can be considered as a single particle average volume). Thus, if the aerosol type is known, comparing of computed $\beta_{1064}^{N=1}$ from Table 1 with observed values β_{1064}, yields the number and volume particle densities as $N = \frac{\beta_{1064}}{\beta_{1064}^{N=1}}$ and $V = N \times V^{N=1}$.

Table 2 summarizes for the three nights from Fig.3, the fluorescence cross sections per a single particle, $\sigma_F^N = \frac{\beta_F}{N}$, and per unit volume, $\sigma_F^V = \frac{\beta_F}{V}$. Values are provided for the altitudes corresponding to the maximum of fluorescence backscattering β_F in elevated layers, where the relative humidity (RH) should be low and hygroscopic effect reduced. Basing on the back trajectory analysis, particles are assumed to be of biomass burning origin for November 30th and January 16th, and of dust origin for February 6-7th. We should remind, however, that our estimations of N (and so σ_F^N) depend on the assumed aerosol type. The particle volume, V, is however a more reliable parameter. For example, if the UR aerosol type is considered, rather than the BB one, the particle number density, N, for November 30th becomes N=21cm^{-3} (instead 63 cm^{-3} for BB) while the total volume remains rather constant (V=0.34 μm^{3}·cm^{-3} instead of 0.37 μm^{3}cm^{-3}). Thus, presentation of cross section per a unit of volume σ_F^V appears more trustable. We should recall also, that comparison of σ_F^V for different aerosol types makes sense only at low RH, when the water uptake effect is small. The results in Table 2 are given for the heights, where RH is below 20%. The fluorescence cross sections σ_F^V for November 30th and January 16th are very close, but for the dust layer (February 6-7th, 2020), the cross section is about a factor 4 lower. From the data presented it is also possible to estimate the spectral differential cross section, $\frac{\sigma_F^V}{\Delta\lambda}$, where $\Delta\lambda$ is the width of the filter transmission band.

It is rather difficult to validate our values of the fluorescence differential cross section. We nevertheless compare them to in situ ground-based fluorescence measurements. Such reference data are available mainly for biological particles (e.g. Pan, 2015). For biological particles, the highest $\frac{d\sigma_F}{d\lambda}$ value, for a single particle with diameter 1.2 μm – 3.0 μm varies in the range (1-100)*10^{-15} cm^{2}sr^{-1}nm^{-1} when stimulating radiation at 365 nm is used (Pan, 2015). Thus, our estimated values look reasonable, keeping in mind that the fluorescence cross section of the biological particles is higher than that of smoke. Still the results presented in the Table 2 should be considered as qualitative and for obtaining quantitative values father studies are needed.

3.2. Fluorescence of aerosol particles within cloud layers

One of the attractive features of the fluorescence technique is the possibility to detect aerosol and derive its content within the cloud layer. However the interpretation of fluorescence measurements in the clouds is rather complicated. Aerosol can be inside the cloud droplets in dissolved or solid state (activated CNN) or in the form of interstitial particles at 100% RH and we need to separate somehow their contribution to the fluorescence signal. The fluorescence backscattering β_F is calculated from the ratio of fluorescence and nitrogen Raman lidar signals and it can be affected by the multiple scattering effects due to significant wavelength separation between Raman and fluorescence components. Thus most trustable observations should be near the cloud base.

The results of measurements in the presence of thin cloud layers on November 13th and 18th are shown in Fig. 4. The backscattering coefficients are given at 532 nm, because in the cloud layers the detector in 1064 nm channel was sometimes saturated. On November 13th, the cloud layers lead to a strong oscillation of β_{532} within 1000 m – 3000 m range. The spikes in β_{532} profile, however, are not followed by synchronous increase of the fluorescence backscattering β_F in the range of 1000—3000 m. On 18th November, the cloud layer within 1500 – 2000 m range exhibit an even stronger elastic backscattering, exceeding 80 Mm^{-1}sr^{-1}, and again, no significant change of fluorescence backscattering is observed. Thus observations in Fig.4 do not reveal unambiguous effect of cloud layers on aerosol fluorescence Moreover, these results clearly indicate the absence of leaks/contamination of elastic scattering in the fluorescence channel.

The situation, however, can be different, when the cloud droplets are formed on the aerosol particles. Fig.5 shows the height – temporal distributions of the lidar signal at 1064 nm and the fluorescence backscattering coefficient on the night 19-20th November 2019. After 21:50 UTC a thin cloud layer starts to form at the top of the PBL resulting in simultaneous increase of β_F. To quantify the influence of cloud water droplet on the fluorescence backscattering, Fig.6a provides profiles of aerosol and fluorescence backscattering coefficients for two temporal intervals 20:00 – 21:30 UTC and 21:30 – 00:30 UTC, prior and after the cloud layer formation respectively. Prior to cloud formation the aerosol load is very low, so backscattering is provided only at 1064 nm and to be distinguished at this figure, the value of β_{1064} is multiplied by factor 100. For 20:00 – 21:30 β_{1064} at 1500 m (height where the cloud forms) is about 0.07 Mm^{-1}sr^{-1}. Corresponding value at 532 nm should be about 0.15 Mm^{-1}sr^{-1} (for backscattering Angstrom exponent of 1.0). After the cloud formation the backscattering coefficient is shown at 532 nm, because 1064 nm detector in the cloud layer was overloaded. The β_{532} at 1500 m is of 500 Mm^{-1}sr^{-1}, thus β_{532} increases by a factor of 3000 roughly, while β_F increases by approximately a factor 5.

Similar scenario occurred on the night 23-24th November 2019 (Fig.6b). Prior to the cloud formation (21:00 – 23:00 UTC) the backscattering coefficient at 900 m height is β_{1064}=0.02 Mm^{-1}sr^{-1} (β_{532} should be about 0.02 Mm^{-1}sr^{-1}) and after cloud formation β_{532} increases up to 130 Mm^{-1}sr^{-1}. Thus β_{532} enhancement is of factor of 6500, while β_F again increases about factor 5. The profiles of β_F in Fig.6 prior and after the cloud formation remain the same, below the cloud. It corroborates the suggestion that the cloud was not transported by the air masses with different properties, but the process of water vapor condensation occurs.

We should emphasize, that the enhancement of β_F can not be explained by just insufficient suppression of elastic scattering. The enhancement was observed only inside an aerosol layer, while clouds with similar backscattering coefficients, but outside the aerosol layer, didn't provide the increase of β_{532}. As mentioned above, the fluorescence scattering phase function of water microspheres can have a peak in the backward direction (Veselovskii et al., 2002a), leading to increase of β_F, for a particle dissolved in a droplet, by approximately a factor 2 comparing to a solid particle. This is lower than the observed value, and at a moment we are not capable to identify the mechanisms responsible for β_F enhancement. Just should be mentioned, that in principle, water environment may affect the fluorescence efficiency. For example, the fluorescence cross section of wet bacterial spores is higher than that of dry ones (Kunnil et al., 2004). For insoluble particles the presence of a water shell can lead also to additional increase of the fluorescence, due to the lens effect produced by the droplet. More studies are needed to understand the influence of the water uptake by the particle during cloud formation on the fluorescence backscattering.

One of the objectives of this study was to demonstrate the possibility to monitor aerosol within a cloud by fluorescence. Fig.7 shows the height – temporal distributions of the range corrected lidar signal at 1064 nm and the fluorescence backscattering β_F on November 15th 2019 for 2:45 – 6:15 UTC period. Low cloud layer appears at approximately 2000 m and a signal of aerosol fluorescence is observed within this layer up to 3000 m. The HYSPLIT back trajectory analysis shows that air masses at this height are transported over Atlantic from Canada. The vertical profiles of β_{532} and β_F, integrated over 2:45 – 6:15 temporal interval, are shown in Fig.8a. Fluorescence backscattering is about $0.03*10^{-4}$ $Mm^{-1}sr^{-1}$ at 1500 m and it rises to $0.045*10^{-4}$ $Mm^{-1}sr^{-1}$ at 2000 m, near the cloud base, where RH can be close to 100%. Inside the cloud β_F increases up to $0.07*10^{-4}$ $Mm^{-1}sr^{-1}$ at 3000 m, where elastic backscattering is maximal. Thus total increase of β_F in 1500 – 3000 m range is slightly above a factor 2 and probably can be attributed to the water uptake by the particles. High value of β_F in the cloud is probably due to the contribution of interstitial aerosol particles.

On November 25th 2019 (Fig.8b), a low cloud layer at 850 m leads to increase of β_F by approximately a factor 2, in a similar way as in Fig.6. However, above 1000 m the aerosol content is very low and β_F is below $0.005*10^{-4}$ $Mm^{-1}sr^{-1}$. The sensitivity of the fluorescence measurements can be limited by the fluorescence of the optics in the lidar receiver. The lowest value of β_F observed in our measurements (averaged over several hundred meters height range) was about $0.004*10^{-4}$ $Mm^{-1}sr^{-1}$, thus β_F in Fig.8b can be below the limit of our sensitivity. Above

2000 m strong cloud layer, with maximal value of β_{532} above 100 $Mm^{-1}sr^{-1}$, occurs. Back trajectory analysis demonstrates that air masses at this height are transported over Atlantic from the south of USA. The β_F in the cloud, averaged over 2200 – 2750 range, is about $0.006*10^{-4}$ $Mm^{-1}sr^{-1}$, which is significantly lower than in Fig.8a. Thus on 25 November the cloud is less "polluted" by aerosol than on 15 November. The fluorescence signal can be produced by both activated CCN and by interstitial aerosol particle, and at a present stage we are not able to separate their contributions.

Conclusion

In our research we analyzed the feasibility of the fluorescence channel, added to the multiwavelength Mie-Raman lidar, for aerosol characterization. The results obtained, demonstrate that the use of an interference filter for selection the part of the fluorescence spectrum allows efficient lidar operation. In particular, LILAS lidar with the interference filter of 44 nm width in the fluorescence channel, was able to detect fluorescence signal from weak aerosol layers ($\beta_{1064} < 0.02$ $Mm^{-1}sr^{-1}$) up to 5000 m. During the experiment the fluorescence capacity $G_F = \frac{\beta_F}{\beta_{1064}}$ of aerosol at condition of low RH varied through the $(0.6 - 2.5)\times 10^{-4}$ range, being the highest for the smoke and the lowest for the dust particles.

The lidar measurements, in principle, allow to get the information about the aerosol fluorescence cross section in the elevated aerosol layers. For several atmospheric situations the rough estimations of the fluorescence cross section were performed in this study and the results obtained look reasonable, comparing with published values for biological particles. Still these results should be taken as preliminary and the next important step in quantification of the fluorescence measurements will be the system calibration, using a lamp with known spectrum. As well, more deep comparison of σ_F obtained from the laboratory and lidar measurements, for different aerosol types, is needed for validation. The fluorescence and multiwavelength Mie-Raman lidar techniques are complimentary: the multiwavelength lidar allows aerosol typing and estimation of the particle number and volume densities, that are later used to derive the fluorescence cross sections from observed β_F. The fluorescence measurements, in turn, help to improve the aerosol classification. The synergy of fluorescence and multi-wavelength lidar techniques was not realized in this study, due to too low aerosol loading in November – February period. However, we plan new experiments during Spring – Summer season, when AOD is larger in Lille.

Results presented demonstrate also, that the fluorescence technique can be used to monitor the aerosol particles inside the cloud (at least near the cloud base, if penetration depth of the laser radiation is small), which is important in the study of aerosol – cloud interaction. However to get quantitative information about particle properties we need deeper understanding of influence of the water uptake by the particles on the fluorescence efficiency. In particular, in the clouds formed at the top or inside the aerosol layer, an increase of the fluorescence backscattering coefficient up to factor 5) was observed, and at a moment we are not able to specify the processes behind this enhancement.

In coming studies we plan additional modifications of the lidar. In particular, we consider the possibility to add second fluorescence channel near 550 nm, which should improve selectivity of the fluorescence technique to different aerosol types. The water vapor channel will be returned back to the system, which is essential for the study of particle hygroscopic growth. Collocated measurements of the microwave radiometer of the Laboratoire d'optique atmosphérique will be used to derive the RH profiles.

Acknowledgments

The authors are grateful to Service National d’Observation PHOTONS/AERONET-EARLINET from CNRS-INSU, France; to ACTRIS-2 program under the European Union’s Horizon 2020 research and innovation programme under grant agreement no. 654109; to Région Hauts-de-France and the Ministère de l’Enseignement Supérieur et de la Recherche (CPER Climibio); and to IDEAS+/ESA Programme for supporting this research. We are also very grateful to Albert Ansmann and Yongle Pan for numerous useful discussions.

Table 1. Parameters of the biomass burning (BB), URban and DUst particles used in the model. The volume $V^{N=1}$ and backscattering coefficient $\beta_{1064}^{N=1}$ are given for a single particle (N=1).

Type	$r_{V,f}$ µm	$r_{V,c}$ µm	σ_f	σ_c	$\frac{C_{V,f}}{C_{V,c}}$	CRI $_{1064}$	$V^{N=1}$ $\mu m^3/cm^3$	$\beta_{1064}^{N=1}$ $Mm^{-1}sr^{-1}$
BB	0.12	3.95	0.4	0.75	1.32	1.51-i.0.02	5.91E-3	1.58E-4
URban	0.175	3.275	0.38	0.75	2.5	1.4-i0.003	1.61E-2	4.69E-4
DUst	0.12	2.32	0.4	0.6	0.05	1.56- i0.001	7.6E-2	2.83E-3

Table.2. The aerosol parameters in elevated layers for three measurement sessions from Fig.3, including the fluorescence β_F and aerosol β_{1064} backscattering coefficients, number N and volume V particle densities, the differential fluorescence cross sections per a single particle $\frac{\sigma_F}{N}$ and per unit volume $\frac{\sigma_F}{V}$, together with spectral density $\frac{\sigma_F}{V\Delta\lambda}$.

Date	Height km	β_F, $Mm^{-1}sr^{-1}$	β_{1064}, $Mm^{-1}sr^{-1}$	N, cm^{-3}	V, $\mu m^3 cm^{-3}$	$\frac{\sigma_F}{N}$, 10^{-15} $cm^2 sr^{-1}$	$\frac{\sigma_F}{V}$, 10^{-13} $cm^2 sr^{-1} \mu m^{-3}$	$\frac{\sigma_F}{V\Delta\lambda}$, 10^{-15} $cm^2 sr^{-1} \mu m^{-3} nm^{-1}$
30 Nov	4.0	3.0E-6	0.010	63	0.37	0.48	0.81	1.84
16 Jan	5.0	4.88E-6	0.013	82	0.60	0.48	0.81	1.84
6-7 Feb	2.9	5.63E-6	0.096	34	2.58	2.18	0.22	0.5

References

Alexandrov, M. and Mishchenko, M.: Information content of bistatic lidar observations of aerosols from space, Opt. Expr. 25, 134-150, 2017.

Ansmann, A., Riebesell, M., Wandinger, U., Weitkamp, C., Voss, E., Lahmann, W., and Michaelis, W.: Combined Raman elastic-backscatter lidar for vertical profiling of moisture, aerosols extinction, backscatter, and lidar ratio, Appl.Phys.B, *55*, 18-28, 1992.

Burris, J., McGee, T.J., Heaps, W.: UV Raman cross sections in nitrogen, Appl. Spectroscopy 46, 1076, 1992.

Burton, S. P., Ferrare, R. A., Hostetler, C. A., Hair, J. W., Rogers, R. R., Obland, M. D., Butler, C. F., Cook, A. L., Harper, D. B., and Froyd, K. D.: Aerosol Classification of Airborne High Spectral Resolution Lidar Measurements – Methodology and Examples, Atmos. Meas. Tech., 5, 73–98, doi:10.5194/amt-5-73-2012, 2012.

Burton, S. P., Chemyakin, E., Liu, X., Knobelspiesse, K., Stamnes, S., Sawamura, P., Moore, R. H., Hostetler, C. A., and Ferrare, R. A.: Information content and sensitivity of the 3β+2α lidar measurement system for aerosol microphysical retrievals, Atmos.Meas. Tech., 9, 5555–5574, 2016.

Dubovik, O., Holben, B., Eck, T.F., Smirnov, A., Kaufman, Y.J., King, M.D., Tanre, D., Slutsker, I.: Variability of absorption and optical properties of key aerosol types observed in worldwide locations, J. Atmos. Sci., 59, 590–608, 2002.

Dubovik, O., Sinyuk, A., Lapyonok, T., Holben, B.N., Mishchenko, M., Yang, P., Eck, T.F., Volten, H., Munoz, O., Veihelmann, B., van der Zande, W.J., Leon, J.-F., Sorokin, M., Slutsker, I.: Application of spheroid models to account for aerosol particle nonsphericity in remote sensing of desert dust, *J. Geophys. Res*., 111, D11208, doi:10.1029/2005JD006619, 2006.

Hill, S. C., Williamson, C. C., Doughty, D. C, Pan, Y.-L., Santarpia, J. L., Hill, H. H.: Size-dependent fluorescence of bioaerosols: Mathematical model using fluorescing and absorbing molecules in bacteria, J. Quant. Spectr. Radiat. Trans., 157, 54–70, 2015.

Horvath, H., Gunter, R. L., and Wilkison, S. W.: Determination of the coarse mode of the atmospheric aerosol using data from a forward-scattering spectrometer probe, Aerosol Sci. Technol., 12, 964–980, 1990.

Hu, Q., Goloub, P., Veselovskii, I., Bravo-Aranda, J.-A., Popovici, I., Podvin, T., Haeffelin, M., Lopatin, A. , Dubovik, O., Pietras, C., Huang, X., Torres, B., and Chen, C.: Long-range-transported Canadian smoke plumes in the lower stratosphere over northern France, Atmos. Chem. Phys. 19, 1173 – 1193, 2019. doi.org/10.5194/acp-19-1173-2019.

Huffman, J.A., Perring, A.E., Savage, N.J., Clot, B., Crouzy, B., Tummon, F., Shoshanim, O., Damit, B., Schneider, J., Sivaprakasam, V., Zawadowicz, M.A., Crawford, I., Gallagher, M., Topping, D., Doughty, D.C., Hill, S.C., Pan, Y.: Real-time sensing of bioaerosols: Review and current perspectives, Aerosol Science and Technology, 2019. DOI: 10.1080/02786826.2019.1664724

Immler, F., Engelbart, D., Schrems, O.: Fluorescence from atmospheric aerosol detected by a lidar indicates biogenic particles in the lower stratosphere, Atmos. Chem. Phys. 5, 345–355, 2005.

Kerker, M., and Druger, S. D.: Raman and fluorescent scattering by molecules embedded in spheres with radii up to several multiples of the wavelength, Appl. Opt. 18**,** 1172–1179, 1979.

Klett J.D., "Lidar inversion with variable backscatter/extinction ratios", Appl.Opt. 24, 1638-1643, 1985.

Kunnil, J., Swartz, B., Reinisch, L.: Changes in the luminescence between dried and wet bacillus spores, Appl. Opt. 43, 5404 – 5409, 2004.

Li, B., Chen, S., Zhang, Y., Chen, H., Guo, P.: Fluorescent aerosol observation in the lower atmosphere with an integrated fluorescence-Mie lidar, J. Quant. Spectr. Rad. Transf., 227, 211–218, 2019.

Luís Guerrero-Rascado, J., Amiridis, V., Kokkalis, P., Apituley, A., Baars, H., Schwarz, A., Wandinger, U., Binietoglou, I., 660 Nicolae, D., Bortoli, D., Comerón, A., Rodríguez-Gómez, A., Sicard, M., Papayannis, A. and Wiegner, M.: An automatic observation-based aerosol typing method for EARLINET, Atmos. Chem. Phys., 18, 15879–15901, doi:10.5194/acp-18-15879-2018, 2018.

Miyakawa, T., Kanaya, Y., Taketani, F., Tabaru, M., Sugimoto, N., Ozawa, Y., and Takegawa, N.: Ground-based measurement of fluorescent aerosol particles in Tokyo in the spring of 2013: potential impacts of nonbiological materials on autofluorescence measurements of airborne particles, J. Geophys. Res. Atmos., 120, 1171–1185, 2015, doi:10.1002/2014JD022189.

Müller, D., Wandinger, U., and Ansmann, A.: Microphysical particle parameters from extinction and backscatter lidar data by inversion with regularization: theory, Appl. Opt. 38, 2346-2357, 1999.

Pan, Y.L., Hill, S.C., Wolf, J.P., Holler, S., Chang, R.K., Bottiger, J.R.: Backward-enhanced fluorescence from clusters of microspheres and particles of tryptophan, Appl. Opt. 41, 2994-2999, 2002.

Pan, Y.-L., Pinnick, R.G., Hill, S.C., Rosen, J.M., and Chang, R.K.: Single-particle laser-induced-fluorescence spectra of biological and other organic-carbon aerosols in the atmosphere: Measurements at New Haven, Connecticut, and Las Cruces, New Mexico, J. Geophys. Res., 112, D24S19, doi:10.1029/2007JD008741, 2007.

Pan, Y.-L.: Detection and characterization of biological and other organic-carbon aerosol particles in atmosphere using fluorescence, J. Quant. Spectr. Radiat. Trans. 150, 12–35, 2015

Rao, Z., He, T., Hua D, Wang, Y., Wang, X., Chen, Y., Le J.: Preliminary measurements of fluorescent aerosol number concentrations using a laser-induced fluorescence lidar, Appl. Opt. 57, 7211-7215, 2018.

Reichardt, J.: Cloud and aerosol spectroscopy with Raman lidar, J. Atm. Ocean. Tech., 31, 1946-1963, 2014.

Reichardt, J., Leinweber, R., Schwebe, A.: Fluorescing aerosols and clouds: investigations of co-existence, Proceedings of the 28th ILRC, Bucharest, Romania, 25-30 June, 2017.

Saito, Y., Ichihara, K., Morishita, K., Uchiyama, K., Kobayashi, F., Tomida, T.: Remote detection of the fluorescence spectrum of natural pollens floating in the atmosphere using a laser-induced-fluorescence spectrum (LIFS) lidar, Remote Sens., 10, 1533, 2018. doi:10.3390/rs10101533.

Schnaiter, M., Linke, C., Mohler, O., Naumann, K. H., Saathoff, H., Wagner, R., Schurath, U., and Wehner, B.: Absorption amplification of black carbon internally mixed with secondary organic aerosol, J. Geophys. Res., 110, D19204, 2005.

Stein, A.F., Draxler, R.R, Rolph, G.D., Stunder, B.J.B., Cohen, M.D., and Ngan, F.: NOAA's HYSPLIT atmospheric transport and dispersion modeling system, Bull. Amer. Meteor. Soc., 96, 2059-2077, 2015. http://dx.doi.org/10.1175/BAMS-D-14-00110.1

Sugimoto, N., Huang, Z., Nishizawa, T., Matsui, I., Tatarov, B.: Fluorescence from atmospheric aerosols observed with a multichannel lidar spectrometer," Opt. Expr. 20, 20800-20807, 2012.

Tesche, M., Groß, S., Ansmann, A., Müller, D., Althausen, D., Freudenthaler, V., and Esselborn, M.: Profiling of Saharan dust and biomass-burning smoke with multiwavelength polarization Raman lidar at Cape Verde, Tellus B, 63, 649–676, doi:10.1111/j.1600-0889.2011.00548.x, 2011.

Venable, D. D., Whiteman, D. N., Calhoun, M. N., Dirisu, A.O., Connell, R. M., Landulfo, E.: Lamp mapping technique for independent determination of the water vapor mixing ratio calibration factor for a Raman lidar system, Appl. Opt., 50, 4622 - 4632, 2011.

Veselovskii, I., Griaznov, V., Kolgotin, A., Whiteman, D.: “Angle- and size-dependent characteristics of incoherent Raman and fluorescent scattering by microsoheres 2.: Numerical simulation”, Appl. Opt. 41, 5783-5791, 2002a.

Veselovskii I., Kolgotin, A., Griaznov, V., Müller, D., Wandinger, U., Whiteman, D.: Inversion with regularization for the retrieval of tropospheric aerosol parameters from multi-wavelength lidar sounding, Appl.Opt. 41, 3685-3699, 2002b.

Veselovskii, I., Goloub, P., Hu, Q., Podvin, T., Whiteman, D. N., Korenskiy, M., Landulfo, E.: Profiling of CH4 background mixing ratio in the lower troposphere with Raman lidar: a feasibility experiment., Atmos. Meas. Tech. 12, 119–128, 2019. doi.org/10.5194/amt-12-119-2019.

Veselovskii, I., Hu, Q., Goloub, P., Podvin, T., Korenskiy, M., Derimian, E., Legrand, M., Castellanos, P.: Variability of Lidar-Derived Particle Properties Over West Africa Due to Changes in Absorption: Towards an Understanding. Atm. Chem. Phys., 20, 6563-6581, 2020.

Whiteman, D. N., B. Demoz, P. Di Girolamo, J. Comer, I. Veselovskii, K. Evans, Z. Wang, M. Cadirola, K. Rush, G. Schwemmer, B. Gentry, S. H. Melfi, B. Mielke, D. Venable, T. Van Hove, “Raman Water Vapor Lidar Measurements During the International H2O Project. I. Instrumentation and Analysis Techniques”, J. Atmos. Oceanic Technol., 23, 157-169, 2006.

Figures

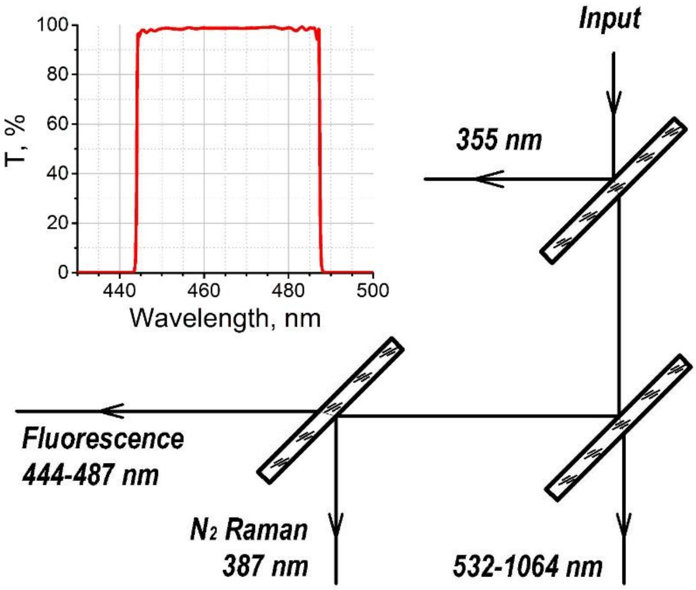

Fig.1 Optical scheme of the elastic, Raman and fluorescence backscatters separation together with transmission curve of the interference filter in the fluorescence channel.

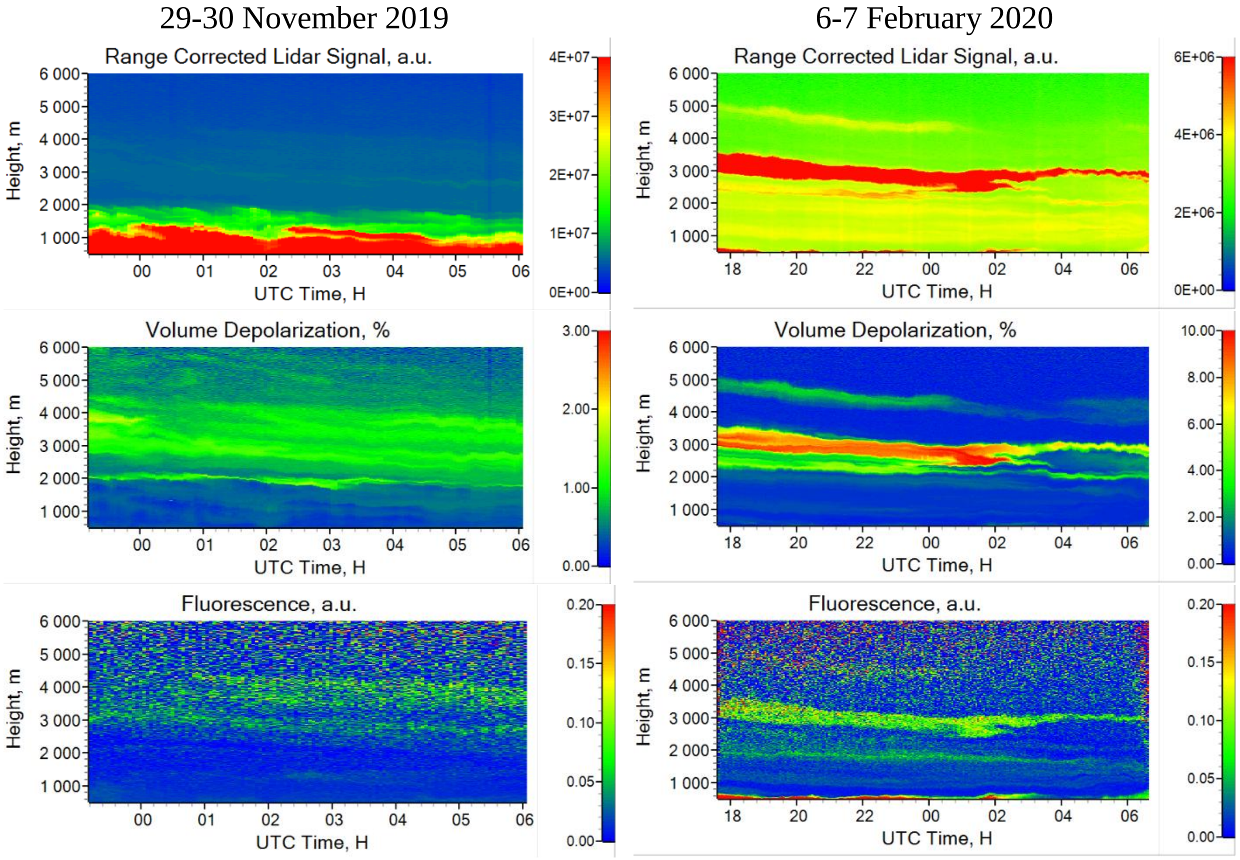

Fig.2. The range corrected lidar signal at 1064 nm, volume depolarization ratio δ_{1064} and fluorescence backscattering measured at Lille, on 29-30 November 2019 (on the left) and 6-7 February 2020 (on the right).

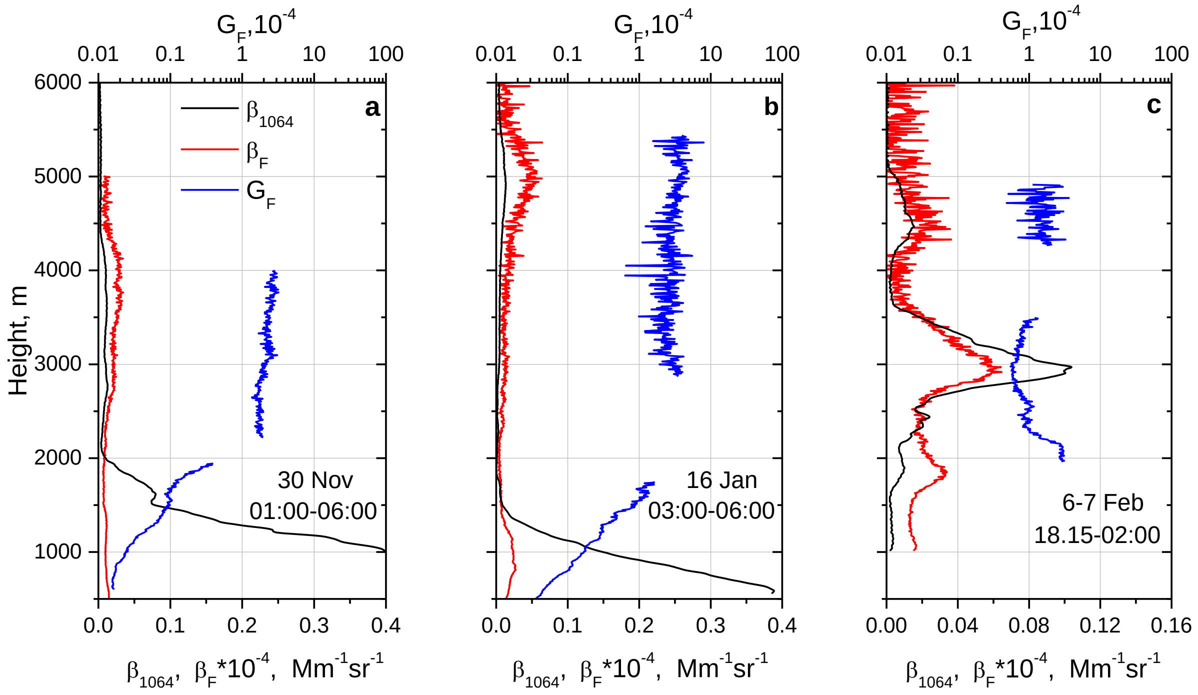

Fig.3 Vertical profiles of aerosol (β_{1064}) and fluorescence (β_F) backscattering coefficients together with the fluorescence capacity (G_F) on (a) 30 November 2019, (b) 16 January 2020 and (c) 6-7 February 2020.

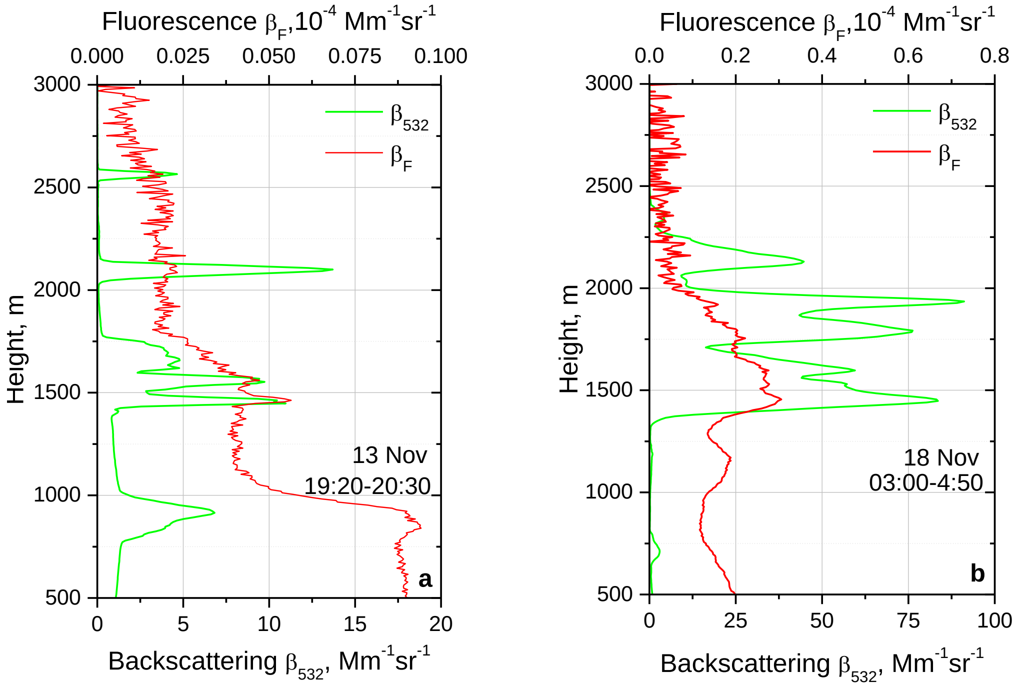

Fig.4. Aerosol (β_{532}) and fluorescence (β_F) backscattering coefficients on 13 and 18 November 2019.

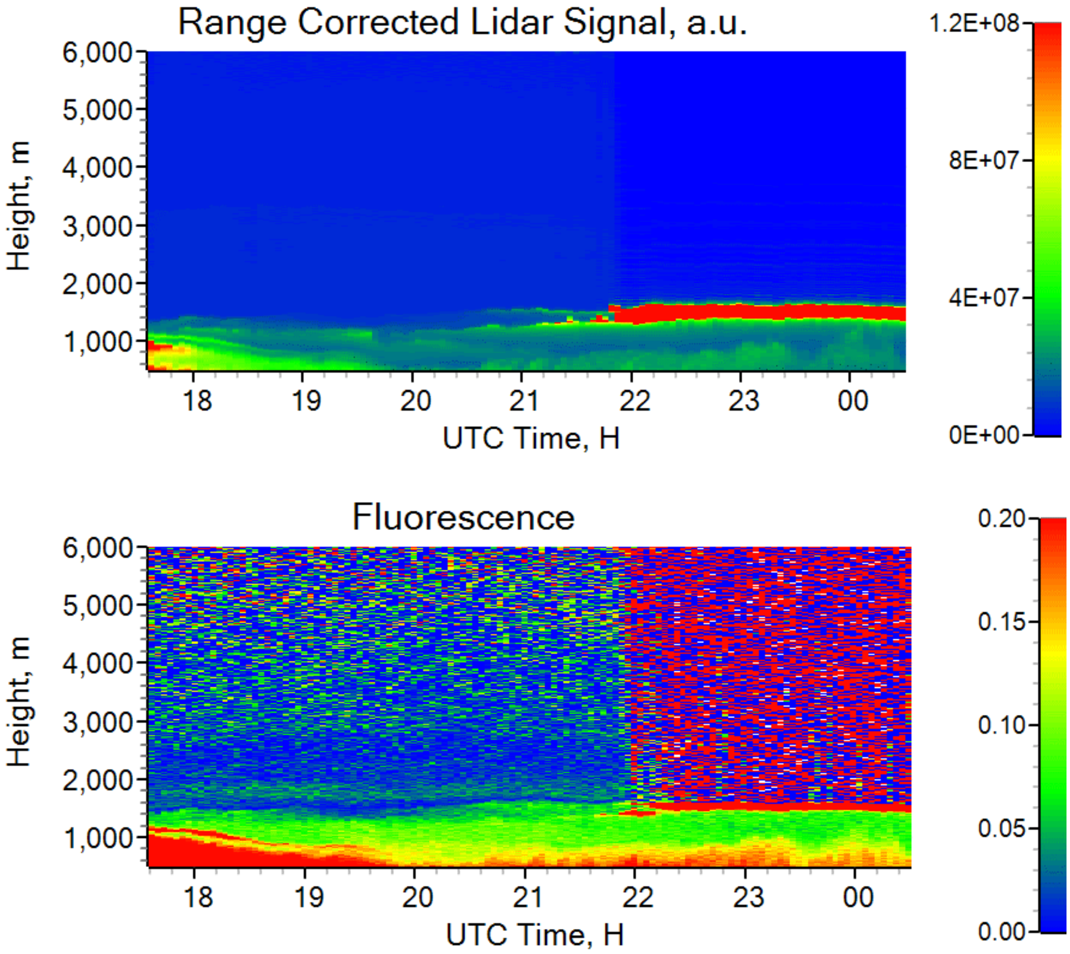

Fig.5. Height-temporal distribution of the range corrected lidar signal at 1064 nm and fluorescence backscattering coefficient β_F (in arbitrary units) on 19-20 November 2019.

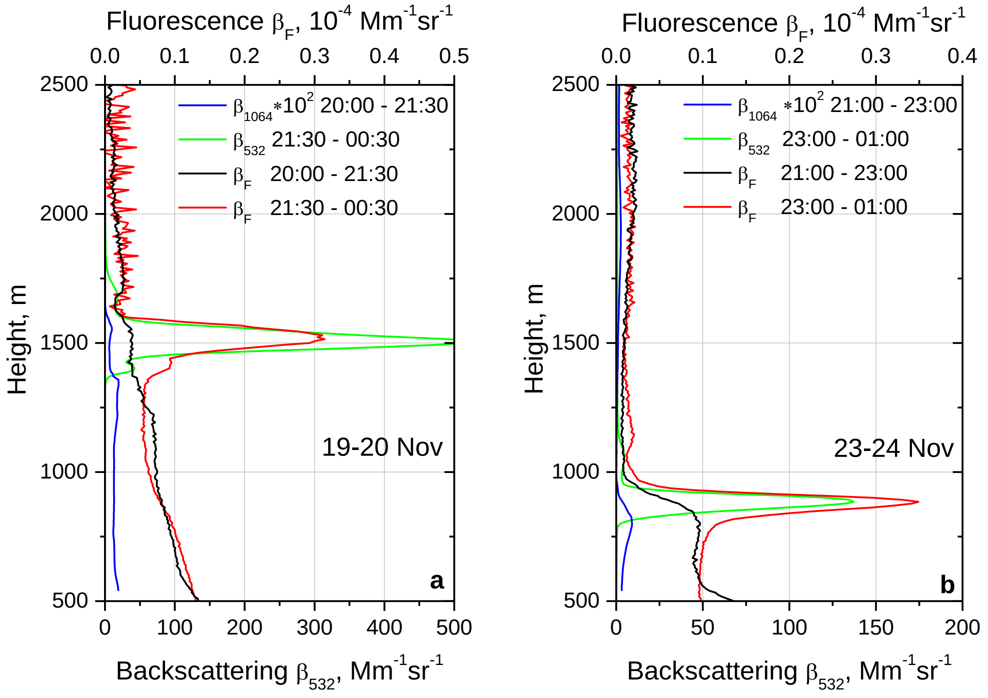

Fig.6. Aerosol and fluorescence backscattering coefficients on (a) 19-20 and (b) 23-24 November 2019 for two time intervals: prior and after cloud formation. Backscattering coefficient β_{1064} prior to cloud formation is low, so it is multiplied by factor 100 to be distinguished at this figure.

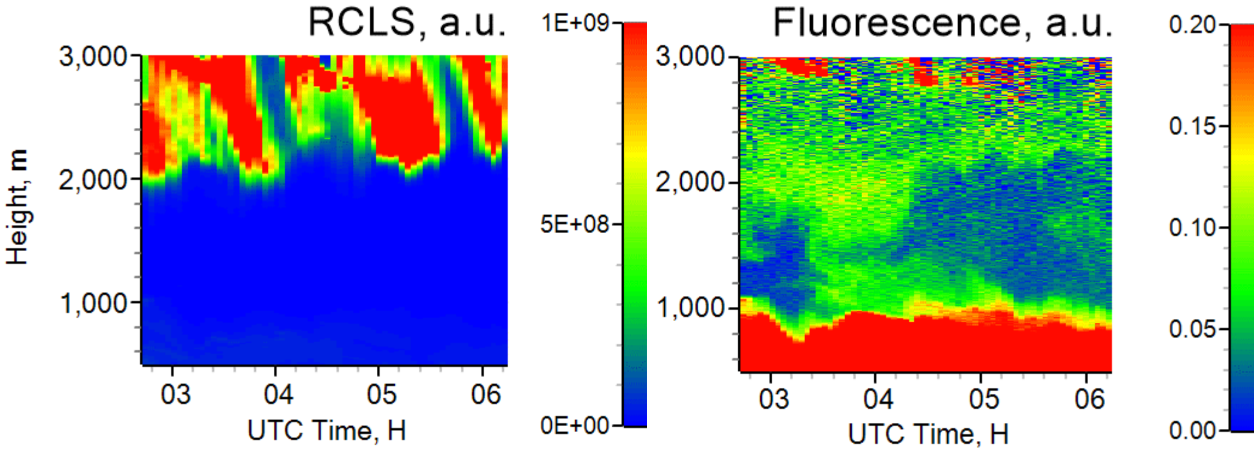

Fig.7. Height-temporal distribution of the range corrected lidar signal (RCLS) at 1064 nm and the fluorescence backscattering coefficient on 15 November 2019.

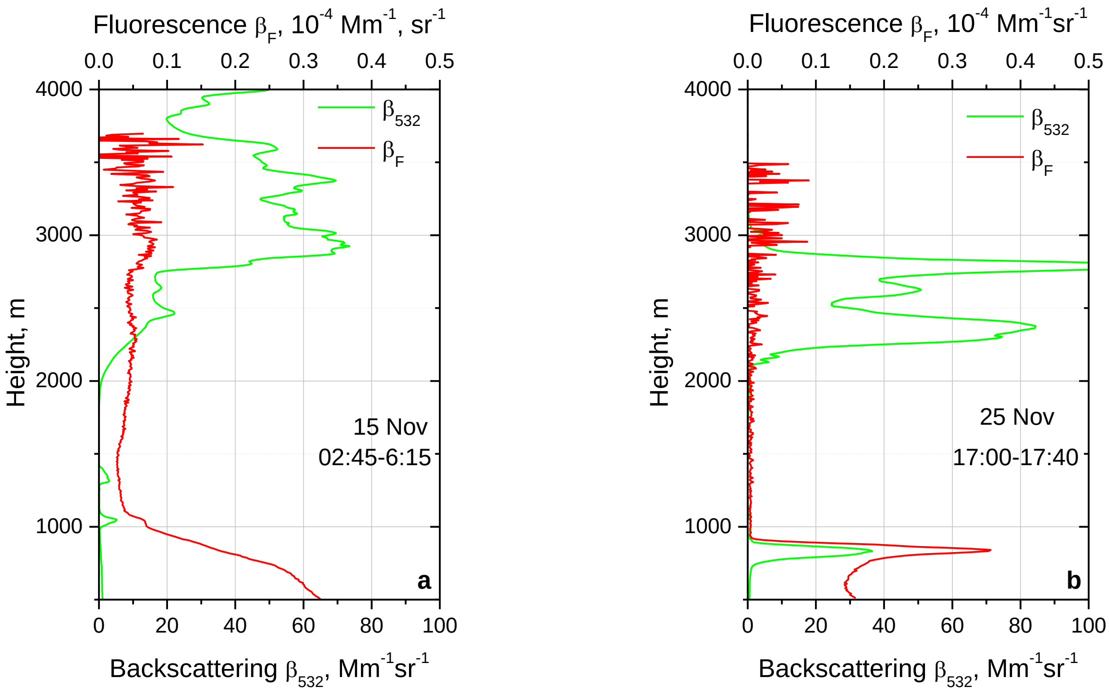

Fig.8. Aerosol (β_{532}) and fluorescence (β_F) backscattering coefficients on (a) 15 and (b) 25 November 2019.